Int. J. Nano Dimens., 12 (2): 135-144, Spring 2021

ORIGINAL ARTICLE

Cubane cluster surface for pyrimidine nucleobases relaxation: DFT approach

Mahmoud Mirzaei [1, 2, *], ***Nasser Hadipour*** [3], ***Oğuz Gülseren*** [4]

[1] *Bioinformatics Research Center, School of Pharmacy and Pharmaceutical Sciences, Isfahan University of Medical Sciences, Isfahan, Iran*
[2] *Biosensor Research Center, School of Advanced Technologies in Medicine, Isfahan University of Medical Sciences, Isfahan, Iran*
[3] *Department of Chemistry, Tarbiat Modares University, Tehran, Iran*
[4] *Department of Physics, Bilkent University, Ankara, Turkey*

Received 30 October 2020; revised 29 November 2020; accepted 20 December 2020; available online 27 December 2020

Abstract

Density functional theory (DFT) approach was employed to investigate relaxation processes of each of pyrimidine nucleobases (NBs); cytosine (C), thymine (T) and uracil (U), at the Cubane Cluster Surface (CCS). The main idea was about providing a material for recognition of NBs, in which a nanostructure form of cubane (CCS) was first generated by optimization process. In the next step, relaxation processes of each of NBs at the surface were investigated to examine the function of such system for NBs recognition. The results indicated that the electronic based molecular properties could work as proper parameters for recognizing such molecular system, in which energy gap (EG) could be referred for the purpose. Measuring EG could help to recognize the complexes of CCS-C, CCS-T and CCS-U from each other. Strength of such complex formations was investigated using values of binding energy (BE); CCS-U > CCS-C > CCS-T. Total results of EG, BE and additional atomic scale properties indicated that the investigated CCS could work very well to recognize U as the characteristic NB of RNA.

Keywords: *Cluster; Cubane; DFT; Nucleobase; Recognition.*

How to cite this article

Mirzaei M., Hadipour N., Gülseren O. Cubane cluster surface for pyrimidine nucleobases relaxation: DFT approach. Int. J. Nano Dimens., 2021; 12(2): 135-144.

INTRODUCTION

Carbon nanotube (CNT) innovation has raised considerable efforts for development of various aspects of this novel material in addition to innovate other related ones [1]. CNT itself and its modification showed wonderful features very much useful for different applications and specified purposes [2]. The benzene-architecture of CNT raised the idea to find other spherical and cyclic structures to innovate other nanostructures [3]. Buckyball (C_{60}) is a good example of such case, which is consisting of mixture of cyclic hexagonal and pentagonal carbon structures [4]. Surveying through literature shows several other examples in shapes and atomic components to be categorized in nanostructures [5]. Cubane (Fig. 1) is a cubic carbon structure, which has been always interesting for researchers because of its unique structural features to work as a single structure or in combination with other structures [6]. Moreover, its modification by functional groups made it useful for some other applications [7]. Previously, possibility of formation of cubane nanostructure was seen as an important topic of literature to have some single standing counterparts [8]. It was shown that linear or cluster forms of cubane complexes could work very well for specific purposes of nanotechnology fields [9]. To this aim, such advantage was investigated

* Corresponding Author Email: *mdmirzaei@pharm.mui.ac.ir*

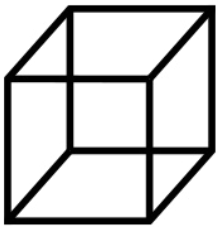

Fig. 1. Cubane (ChemSpider ID: 119867).

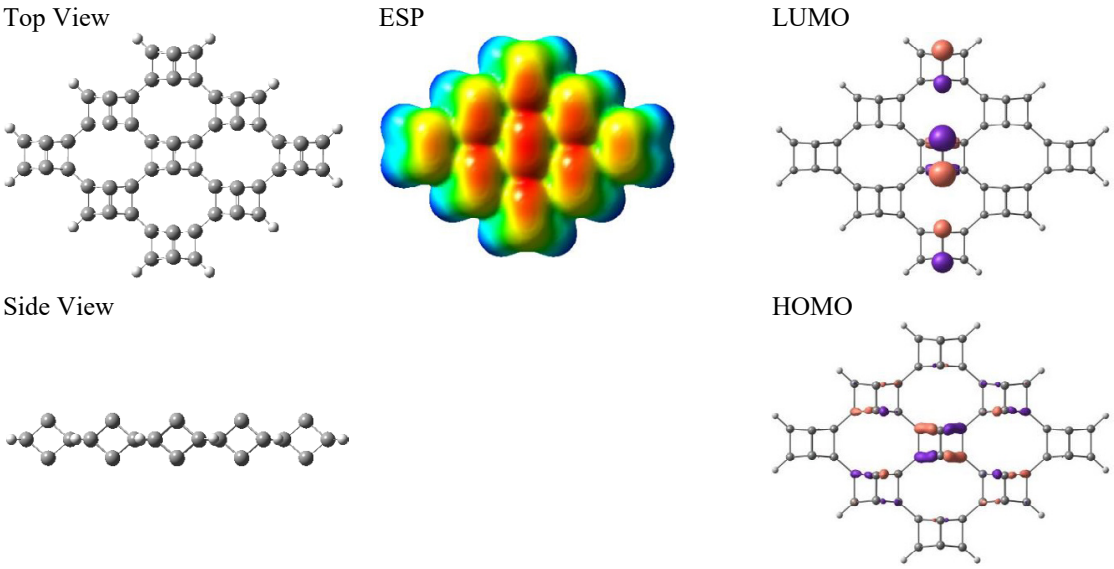

Fig. 2. Cubane Cluster Surface (CCS), ESP surface and LUMO/HOMO distribution patterns.

in this work to see the formation possibility of Cubane Cluster Surface (CCS) (Fig. 2) in addition to relaxation of nucleobases at such surface (Figs. 3 and 4). The pioneering work of DNA recognition by Watson and Crick in 1953 leaded huge number of research works on characterizing such building blocks of living systems [10]. The structures are very well known now, but their separation is still a difficult task to be done [11]. Moreover, formation of complexes of nanostructures and nucleobases could be expected to work in drug delivery purposes [12]. Nucleobases could be involved in the structures of viruses to damage living systems in addition to their benefits; therefore, they should be recognized to prevent such activity [13]. HIV and COVID-19 are only few examples of such biological disasters to human life, which are both caused by nucleobase-included viruses and their recognition is a must [14-16]. Pyrimidine nucleobases include cytosine (C), thymine (T) and uracil (U) (Fig. 3) consisting similar heterocyclic structure in addition to small difference in some of functional groups [17-19]. Such small difference made this pyrimidine nucleobases working differently in living systems; T is the characteristic nucleobase of DNA whereas U is the characteristic nucleobase of RNA [18, 19]. Therefore, it is an important task to have such useful detector for recognizing small differences of structures for nucleobases. Two other nucleobases are adenine and guanine belonging to purine family completely different from pyrimidine nucleobases [20]. Interactions of biological molecules and nucleobases with nanostructures have been always interesting for researchers of various filed to evaluate novel applications of complex formation of such materials [21-25]. In this work, the investigation was focused on recognition of pyrimidine nucleobases for purposes of separation of such DNA and RNA NBs.

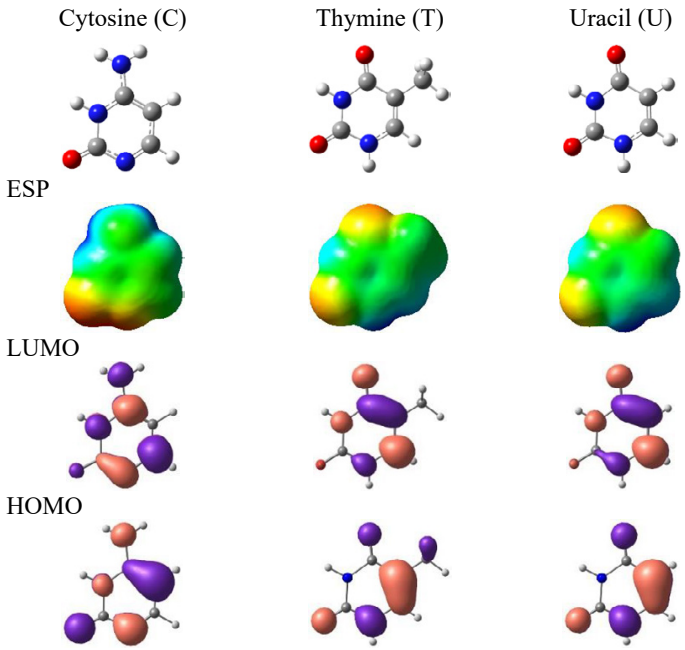

Fig. 3. Pyrimidine nucleobases (optimized structures, ESP surfaces and LUMO/HOMO distribution patterns).

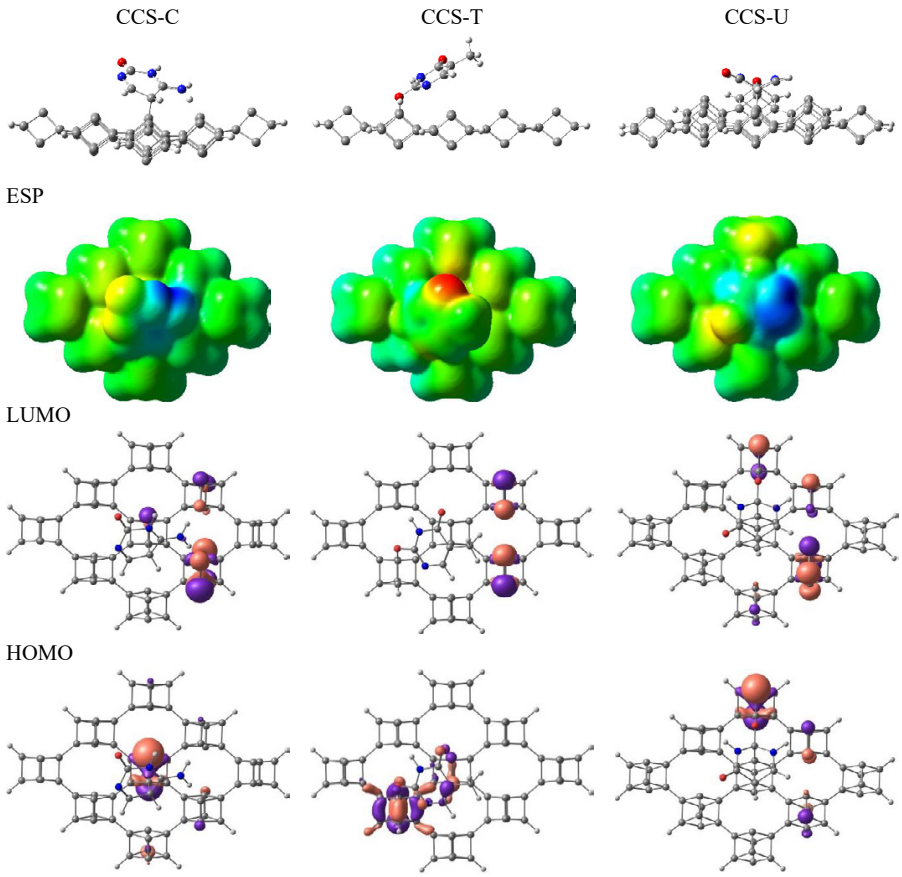

Fig. 4. CCS-NB complexes (optimized structures, ESP surfaces and LUMO/HOMO distribution patterns).

Table 1. Optimized molecular properties*.

Property	CCS	CCS-C	C	CCS-T	T	CCS-U	U
LUMO eV	-4.28	-4.47	-0.94	-4.26	-1.02	-4.41	-1.17
HOMO eV	-6.34	-5.22	-5.98	-6.04	-6.56	-4.88	-6.88
EG eV	2.06	0.75	5.04	1.78	5.54	0.47	5.71
DM Debye	0	6.93	7.84	1.58	4.13	6.32	4.26
BE eV	N/A	-10.01	N/A	-9.51	N/A	-16.11	N/A
CCS-NB Å	N/A	1.54	N/A	1.39	N/A	1.42	N/A

* See Figs. 2-4 for models details. EG = LUMO-HOMO; BE = E_{CCS-NB}-E_{CCS}-E_{NB}.

Within this work, formation of CCS was investigated to be considered as a surface for relaxation of each of pyrimidine nucleobases (C, T and U) (Fig. 4). This work was targeted due to importance of recognition activity of nanostructures for nucleobases. To this aim, quantum mechanical calculations were performed to generate the investigated structures for further examinations. The main problem of this work was oriented to see the possibility of CCS formation for recognizing pyrimidine nucleobase. In addition to crucial experimental measurements, theoretical works could provide insightful information to validate ideas of molecular systems for further developments [26].

MATERIALS AND METHODS

Density functional theory (DFT) approach was used to perform quantum mechanical calculations at the level of B3LYP exchange-correlation functional and 6-31G* standard basis set as implemented in the Gaussian program [27]. The importance of DFT approach is based on its capability for generating reliable results especially for complicated chemical systems at the atomic and molecular scale [28, 29]. The phenomena are based on electron density distribution to obtain the energy of molecular system [30]. The single-standing CCS was generated from the original cubane (Figs. 1 and 2) through geometry optimization processes. Additionally, each singular C, T and U nucleobases (NBs) (Fig. 3) were optimized to have minimum-energy structures for involving in complex formations with CCS. In the next step, complex formations of CCS-NB were investigated by allowing both structures freely interact with each other (Fig. 4). Grimme's dispersion correction (GD2) was included for the calculations of CCS-NB complexes [31]. By doing such calculations, energy levels of the lowest unoccupied and the highest occupied molecular orbitals (LUMO and HOMO), energy gap (EG), dipole moment (DM), binding energy (BE) and the nearest distance of CCS-NB counterparts in complexes were evaluated (Table 1). Moreover, the electrostatic potential (ESP) surfaces and the LUMO and HOMO distribution patterns were presented to show the surfaces properties and the orbital features of whole investigated systems (Figs. 2-4). Moreover, infrared spectra (IR) were calculated for all the investigated models to see the variations of such systems in the singular and complex structures (Fig. 5). To see the effects of such complex formations of CCS-NB on the atomic properties of C, T and U, quadrupole coupling constants (QCC) were evaluated for the nitrogen and oxygen atoms of NBs in singular and complex structures (Table 2) [32]. By benefits of computer-based studies to examine features of complex systems at the molecular/atomic scales [33-36], this work was performed to examine the relaxation processes of each of C, T and U NBs at the CCS nanostructure regarding the recognition and detection purposes. Indeed, achieving this purpose could be seen as a possible solution of major problem in the current status of living systems and human life. To characterize the original features of CCS through interactions with NBs, the calculations were performed in isolated gas phase for the pristine system [35], otherwise including solvent media in the calculations could be an important task to see the effects of environment on the interacting system [37]. Moreover, surface modification could be done to see the changes of pristine CCS in the atomic doped or molecular functionalized models [38].

RESULTS AND DISCUSSION

In this work, DFT computations were performed to investigate relaxation of pyrimidine NBs (C, T and U) at the CCS nanostructure. To this aim, singular properties of all molecule were investigated first, and their complex formations were investigated next. Table 1 presents the obtained optimized molecular properties, in which a quick look at its

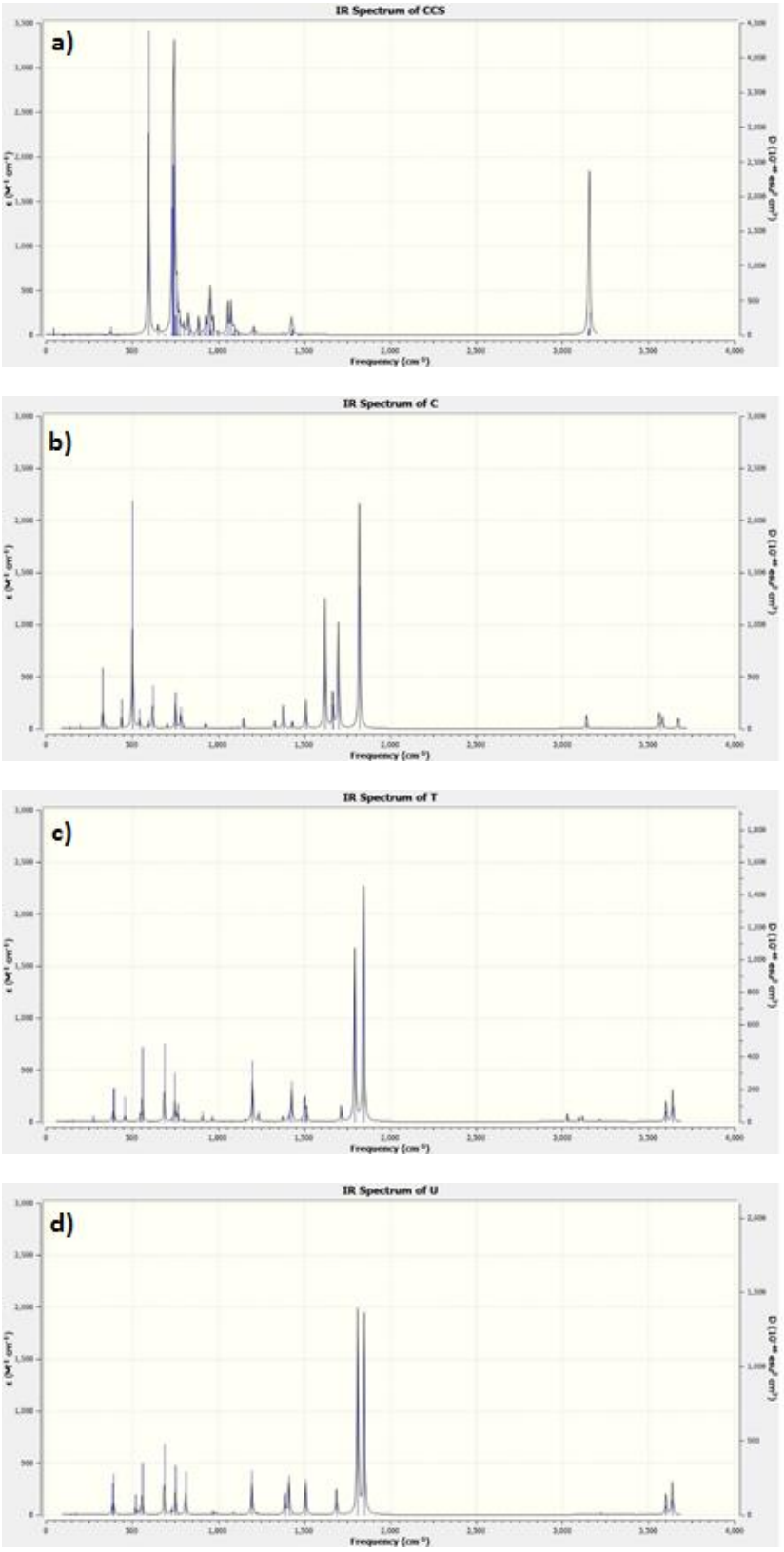

Fig. 5 (a, b, c, d, e, f, g). IR spectra for all singular and complex models.

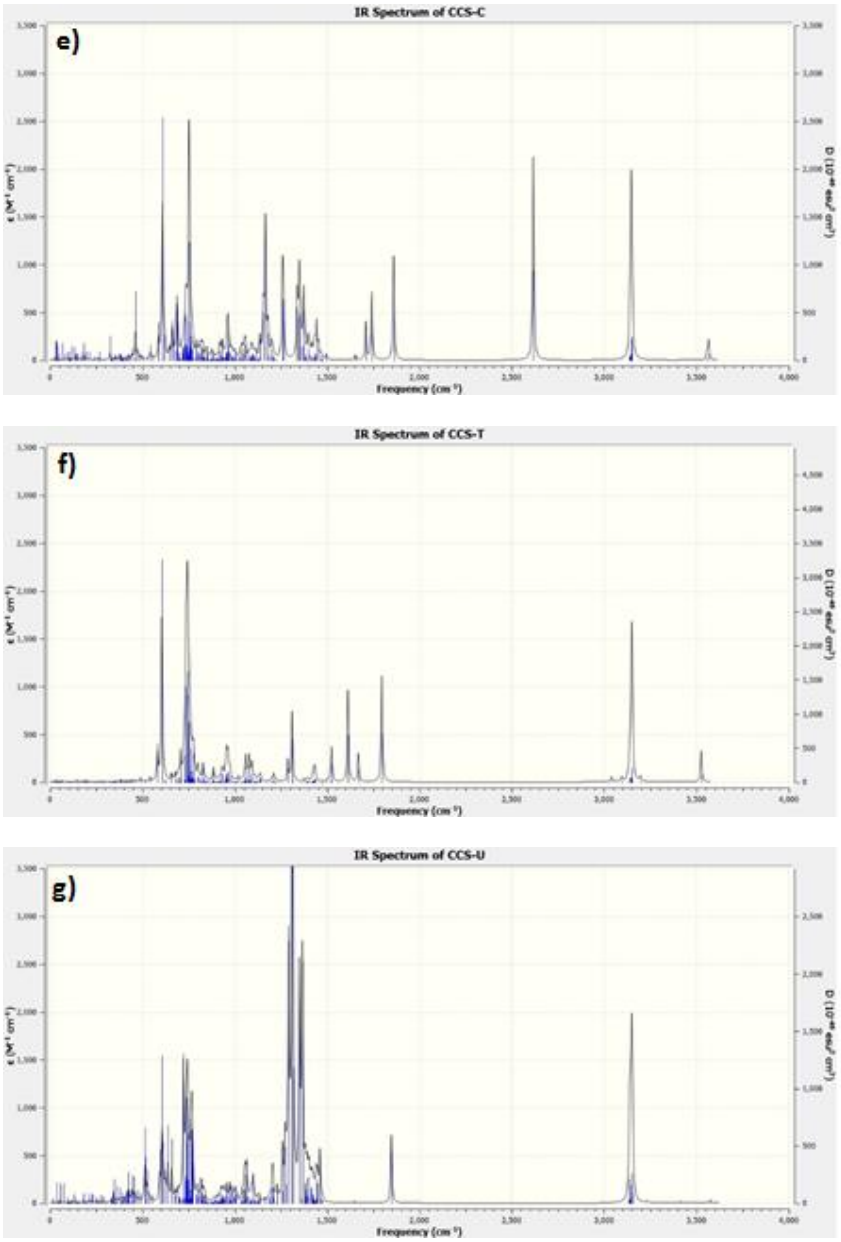

Continued Fig. 5 (a, b, c, d, e, f, g). IR spectra for all singular and complex models.

Table 2. Quadrupole coupling constants (QCC MHz)*.

Atom	CCS-C	C	CCS-T	T	CCS-U	U
N	4.38	3.95	3.46	3.96	1.21	3.91
	3.59	3.58	2.99	3.65	4.52	3.67
	2.39	4.81				
O	10.25	8.81	10.15	8.25	11.18	8.31
			9.08	9.36	9.23	9.44

* See Figs. 2-4 for models details.

results could show different electronic properties for the investigated molecules with significant changes from the singular to complex forms. It is important to note that the stabilized structure of CCS was successfully obtained, in which the obtained layer form could be seen clearly in Fig. 2. By this process, the major material component was available to work as a surface for relaxation of each NB.

It was mentioned earlier that C, T and U NBs are generally similar, but the obtained results showed different electronic properties for these NBs. By such advantage of molecular characterization, it would be possible to recognize such NBs from each other using a material to detect such changes. Changes of LUMO and HOMO for singular NBs, could be used as proper parameters to separate them from each other. Moreover, the values of EG could show such benefit of recognition by a proper surface material. Comparing such electronic properties for the investigated singular and complex models showed that the CCS surface could work as a proper detector for relaxation of NBs. Details of such results could be very well discussed according to magnitude of changes of each parameter from singular to complex forms, in which the obtained magnitudes could show the function of such surface for detection of each of C, T and U NBs. Careful examination of content of Fig. 2 could approve that the size of surface cluster was meaningful for the purpose, in which the LUMO/HOMO distribution patterns were successfully located at the center of surface showing the possible interacting site of CCS far from the edges. Additionally, negative charge was also located at the center of CCS as shown by the red region of ESP surface. The relaxation processes of each of C, T and U NBs at the CCS (Fig. 4) showed that the optimized configurations were located at the surface center of CCS. By such relaxation processes, the localization of typical molecular orbitals were also moved with different magnitudes of changes. The obtained different values of EG (0.75, 1.78 and 0.47 eV for CCS-C, CCS-T and CCS-U) showed that the CCS-NBs complex formations could work for recognizing different NBs. Comparing the values of EG for singular NBs and CCS-NB complexes could show significant changes of such important electronic feature. The largest changes of values for EG were found for U and CCS-U, in which the value was decreased from 5.71 to 0.47 eV with a magnitude of 5.24 eV. The next order was obtained for C and CCS-C, in which the value was decreased from 5.04 to 0.75 eV with a magnitude of 4.29 eV. The last order was for T and CCS-T, in which the value was decreased from 5.54 to 1.78 eV with a magnitude of 3.76 eV. Such different changes of EG from singular NBs to complex forms could yield the detectability of NBs at the surface of CCS. Furthermore, the obtained values of DM also indicated significant effects of such complex formations on the original properties of each of singular CCS and NBs counterparts. This trend could increase hope for recognition purpose of NBs by the investigated CCS material.

Examining the obtained values of BE could indicate that the formation of CCS-U was the most favorable complex formation among the CCS-NBs complexes, in which the value (-16.11 eV) was very much better than other two complexes. Each of CCS-C and CCS-T complex formations could be located at the next orders in the ranking of CCS-NB complex formations. In Fig. 4, it was shown that CCS-U created almost a chelated system, in which the NB counterpart was almost surrounded by the CCS counterpart. This trend could be important regarding the characteristic NB of RNA (U), which could be very well detected by the CCS counterpart. This achievement could distinguish CCS for possible detection of RNA viruses according to show higher interaction tendency to U NB than T and C. As mentioned earlier, general similarity of pyrimidine NBs could yield difficulty for their recognition, in which such CCS-U complex formation could help for the purpose. Although the nearest distance of CCS and NB in the CCS-U was not the shortest one among the complexes, but the relaxation was favorable enough to make it as the most working complex in comparison with other two ones. Comparing these results with other available parallel results in the literature [39, 40] indicated that the investigated CCS could be considered as one of proper surfaces for such function of NBs recognition. The represented ESP surfaces for the CCS-NB complexes (Fig. 4) could yield supportive information for the achievements up to now, in which the blue color at the surface of CCS-U could approve the highest strength of this complex in comparison with other two ones. The red color at the surface of CCS-T could show that the complex was not so much strong regarding other two ones, in which the attached T counterpart could still

have its own electrostatic property. For the CCS-U complex, the ESP surface could show a medium strength complex as indicated earlier by the values of BE. Such achievements were also approved by the obtained IR spectra for the investigated models (Fig. 5), in which the crowded peaks of panels e, f and g of Fig. 5 could show the strength orders of CCS-U>CCS-C>CCS-T. Because of formation of new C-C bonds in the complexes, the populations of crowded peaks were seen especially for stronger complexes, CCS-U. Moreover, such perturbations to the structures of both of CCS (Fig. 5a) and NBs (Fig. 5b, c and d) changed the vibrational modes of the new CCS-NB complex systems different form each of singular forms. Indeed, the vibrational intensity and shifts could be seen because of effects of such structural deformation for the CCS-NB complexes.

Atomic scale properties including QCC for N and O atoms of NBs (Table 2) were calculated to recognize the effects of such complex formations on the characteristic electronic properties of atomic sites. Originally, three different N environments and one O environment were available for C NB versus two different N environments and two different O environments for each of T and U NBs. Therefore, detection of such environments for NBs in singular and complex forms could help to provide information about the effects of such complex formations for the NBs at the atomic scales. The obtained results indicated that the chemical environments at the atomic sites detected the effects of such complex formations. Comparing the results between two structural forms could indicate that the most significant changes of magnitudes of properties for each of N and O atoms from singular form to complex were seen for the CCS-U complex. The value of QCC for one of N atoms changed from 3.91 MHz of singular form to 1.21 MHz of complex form. Additionally, the value of QCC for one of O atoms changed from 8.31 MHz of singular form to 11.18 MHz of complex form. Both of atomic variations of U were significantly different in comparison with each of C and T NBs. Such atomic results could be in agreement with earlier achievement of molecular scale properties, which introduced CCS-U as the most favorable complex.

CONCLUSION

In this DFT work, the relaxation processes of each of C, T and U NBs at the CCS were investigated by the obtained molecular and atomic scale properties. The results indicated that the formation of singular CCS could be seen possible and the obtained layer structure with central localization of LUMO/HOMO approved it. Formation processes of CCS-NB complexes indicated that the CCS could work differently regarding the relaxation of each of NBs, in which the formation of CCS-U complex was the most favorable one among other ones. Furthermore, magnitudes of values of EG indicated that the recognition of such different CCS-NB complexes could be possible for the purpose. To show the strength of complexes, values of BE indicated that the formation of CCS-U could be typically distinguished among other complexes, in which the graphical representation of the optimized complex indicated that the U counterpart was almost chelated by the CCS counterpart. Additionally, the values of QCC atomic scale properties indicated that the changes of chemical environments for N and O atoms of U were very much significant from singular to complex forms, approving the achievement of favorability of CCS-U complex formation. Finally, the investigated CCS counterpart could be available for pyrimidine NBs recognition with the most specific function for detection of U, as the characteristic NB or RNA.

ACKNOWLEDGEMENTS

The support of this work by the research council of Isfahan University of Medical Sciences under grant number 294219 is acknowledged.

CONFLICT OF INTERESTS

There is no conflict of interests for the authors.

REFERENCES

1. Iijima S., (2002), Carbon nanotubes: Past, present, and future. *Physica B.* 323: 1-5.
2. Mirzaei M., Kalhor H. R., Hadipour N. L., (2011), Covalent hybridization of CNT by thymine and uracil: A computational study. *J. Mol. Model.* 17: 695-699.
3. Kulnitskiy B. A., Mordkovich V. Z., Karaeva A. R., Urvanov S. A., Blank V. D., (2020), Cubic and tetragonal maghemite formation inside carbon nanotubes under chemical vapor deposition process conditions. *Fuller. Nanotube. Carbon Nanostruct.* 28: 913-918.
4. Chu D., Liu Y., Li Y., Liu Y., Cui Y., (2020), Journey to the holy grail of coordination saturated Buckyball. *Inorg. Chem. Front*. 142: 7584-7590.
5. Alijani H., Tayyebi S., Hajjar Z., Shariatinia Z., Soltanali S., (2017), Prediction of the Carbon nanotube quality using

adaptive neuro–fuzzy inference system. *Int. J. Nano Dimens.* 8: 298-306.
6. Biegasiewicz K. F., Griffiths J. R., Savage G. P., Tsanaktsidis J., Priefer R., (2015), Cubane: 50 years later. *Chem. Rev.* 115: 6719-6745.
7. Li B. T., Jiang J. J., Li L. L., Peng J., (2020), Thermal stability and detonation character of nitroso-substituted derivatives of cubane. *Mol. Phys.* Article: e1834157.
8. Mansoori G. A., George T. F., Assoufid L., Zhang G., (2007), *Molecular Building Blocks for Nanotechnology: From Diamondoids to Nanoscale Materials and Applications.* Springer Science & Business Media.
9. Huang H. T., Zhu L., Ward M. D., Wang T., Chen B., Chaloux B. L., Wang Q., Biswas A., Gray J. L., Kuei B., Cody G. D., (2020), Nanoarchitecture through Strained molecules: Cubane-derived scaffolds and the smallest carbon nanothreads. *J. Am. Chem. Soc.* 142: 17944-17955.
10. Watson J. D., Crick F. H., (1953), Molecular structure of nucleic acids: A structure for deoxyribose nucleic acid. *Nature.* 171: 737-738.
11. Heller C., (2001), Principles of DNA separation with capillary electrophoresis. *Electrophores.* 22: 629-643.
12. Nikfar Z., Shariatinia Z., (2020), Tripeptide arginyl-glycyl-aspartic acid (RGD) for delivery of Cyclophosphamide anticancer drug: A computational approach. *Int. J. Nano Dimens.* 11: 312-336.
13. Crick F. H., Watson J. D., (1956), Structure of small viruses. *Nature.* 177: 473-475.
14. Gelderblom H. R., Hausmann E. H., Özel M., Pauli G., Koch M. A., (1987), Fine structure of human immunodeficiency virus (HIV) and immunolocalization of structural proteins. *Virolog.* 156: 171-176.
15. Boopathi S., Poma A. B., Kolandaivel P., (2020), Novel 2019 coronavirus structure, mechanism of action, antiviral drug promises and rule out against its treatment. *J. Biomol. Struct. Dyn.* 2020: 1-10.
16. Jiao J., Duan C., Xue L., Liu Y., Sun W., Xiang Y., (2020), DNA nanoscaffold-based SARS-CoV-2 detection for COVID-19 diagnosis. *Biosens. Bioelec.* 167: 112479-112485.
17. Mirzaei M., Elmi F., Hadipour N. L., (2006), A systematic investigation of hydrogen-bonding effects on the 17O, 14N, and 2H nuclear quadrupole resonance parameters of anhydrous and monohydrated cytosine crystalline structures: A density functional theory study. *J. Phys. Chem. B.* 110: 10991-10996.
18. Mirzaei M., Hadipour N. L., Ahmadi K., (2007), Investigation of C–H… OC and N–H… OC hydrogen-bonding interactions in crystalline thymine by DFT calculations of O-17, N-14 and H-2 NQR parameters. *Biophys. Chem.* 125: 411-415.
19. Mirzaei M., (2013), Uracil-functionalized ultra-small (n, 0) boron nitride nanotubes (n= 3–6): Computational studies. *Superlat. Microstruct.* 57: 44-50.
20. Mirzaei M., Kalhor H. R., Hadipour N. L., (2011), Investigating purine-functionalised carbon nanotubes and their properties: A computational approach. *IET Nanobiotechnol.* 5: 32-35.
21. Faramarzi R., Falahati M., Mirzaei M., (2020), Interactions of fluorouracil by CNT and BNNT: DFT analyses. *Adv. J. Sci. Eng.* 1: 62-66.
22. Harismah K., Ozkendir O. M., Mirzaei M., (2020), Lithium adsorption at the C20 fullerene-like cage: DFT approach. *Adv. J. Sci. Eng.* 1: 74-79.
23. Mirzaei M., (2013), Effects of carbon nanotubes on properties of the fluorouracil anticancer drug: DFT studies of a CNT-fluorouracil compound. *Int. J. Nano Dimens.* 3: 175-179.
24. Naderi E., Mirzaei M., Saghaie L., Khodarahmi G., Gulseren O., (2017), Relaxations of methylpyridinone tautomers at the C60 surfaces: DFT studies. *Int. J. Nano Dimens.* 8: 124-131.
25. Mirzaei M., Meskinfam M., Yousefi M., (2012), Covalent hybridizations of carbon nanotubes through peptide linkages: a density functional approach. *Comput. Theor. Chem.* 981: 47-51.
26. Mirzaei M., (2020), Science and engineering in silico. *Adv. J. Sci. Eng.* 1: 1-2.
27. Gaussian 09, Revision D.01, Frisch M. J., Trucks G. W., Schlegel H. B., Scuseria G. E., Robb M. A., Cheeseman J. R., Scalmani G., Barone V., Petersson G. A., Nakatsuji H., Li X., Caricato M., Marenich A., Bloino J., Janesko B. G., Gomperts R., Mennucci B., Hratchian H. P., Ortiz J. V., Izmaylov A. F., Sonnenberg J. L., Williams-Young D., Ding F., Lipparini F., Egidi F., Goings J., Peng B., Petrone A., Henderson T., Ranasinghe D., Zakrzewski V. G., Gao J., Rega N., Zheng G., Liang W., Hada M., Ehara M., Toyota K., Fukuda R., Hasegawa J., Ishida M., Nakajima T., Honda Y., Kitao O., Nakai H., Vreven T., Throssell K., Montgomery J. A., Jr., Peralta J. E., Ogliaro F., Bearpark M., Heyd J. J., Brothers E., Kudin K. N., Staroverov V. N., Keith T., Kobayashi R., Normand J., Raghavachari K., Rendell A., Burant J. C., Iyengar S. S., Tomasi J., Cossi M., Millam J. M., Klene M., Adamo C., Cammi R., Ochterski J. W., Martin R. L., Morokuma K., Farkas O., Foresman J. B., Fox D. J., (2016), Gaussian, Inc., Wallingford CT.
28. Nouri A., Mirzaei M., (2009), DFT calculations of B-11 and N-15 NMR parameters in BN nanocone. *J. Mol. Struct. Theochem.* 913: 207-209.
29. Mirzaei M., (2010), The NMR parameters of the SiC-doped BN nanotubes: A DFT study. *Physica E*. 42: 1954-1957.
30. Parr R. G., (1980), Density functional theory of atoms and molecules. *Horiz. Quant. Chem.*23: 5-15.
31. Grimme S., (2006), Semiempirical GGA-type density functional constructed with a long-range dispersion correction. *J. Comput. Chem.* 27: 1787-1799.
32. Partovi T., Mirzaei M., Hadipour N. L., (2006), The C–H...O hydrogen bonding effects on the 17O electric field gradient and chemical shielding tensors in crystalline 1-methyluracil: A DFT study. *Z. Naturforsch. A.* 61: 383-388.
33. Ozkendir O. M., (2020), Electronic structure study of Sn-substituted InP semiconductor. *Adv. J. Sci. Eng.* 1: 7-11.
34. Yaghoobi R., Mirzaei M., (2020), Computational analyses of cytidine and aza-cytidine molecular structures. *Lab-in-Silico.* 1: 21-25.
35. Mirzaei M., Gülseren O., Hadipour N., (2016), DFT explorations of quadrupole coupling constants for planar 5-fluorouracil pairs. *Comput. Theor. Chem.* 1090: 67-73.
36. Gunaydin S., Alcan V., Mirzaei M., Ozkendir O. M., (2020), Electronic structure study of Fe substituted RuO_2 semiconductor. *Lab-in-Silico.* 1: 7-10.
37. Lashkari M., Arshadi M. R., (2004), DFT studies of pyridine corrosion inhibitors in electrical double layer: Solvent, substrate, and electric field effects. *Chem. Phys.* 299: 131-137.
38. Rad A. S., Mirabi A., Peyravi M., Mirzaei M., (2017), Nickel-decorated B12P12 nanoclusters as a strong adsorbent for SO2 adsorption: Quantum chemical calculations. *Canada. J. Phys.* 95: 958-962.

39. Eslami M., Peyghan A. A., (2015), DNA nucleobase interaction with graphene like BC3 nano-sheet based on density functional theory calculations. *Thin Solid Films.* 589: 52-56.

40. Lee J. H., Choi Y. K., Kim H. J., Scheicher R. H., Cho J. H., (2013), Physisorption of DNA nucleobases on h-BN and graphene: vdW-corrected DFT calculations. *J. Phys. Chem. C.* 117: 13435-13441.